

# Large-Gap Two-Dimensional Topological Insulator in Oxygen Functionalized MXene

Hongming Weng,<sup>1,2,\*</sup> Ahmad Ranjbar,<sup>3</sup> Yunye Liang,<sup>4</sup> Zhida Song,<sup>1</sup> Mohammad Khazaei,<sup>5</sup>  
Seiji Yunoki,<sup>3,6,7</sup> Masao Arai,<sup>5</sup> Yoshiyuki Kawazoe,<sup>4,8</sup> Zhong Fang,<sup>1,2</sup> and Xi Dai<sup>1,2</sup>

<sup>1</sup>*Beijing National Laboratory for Condensed Matter Physics,  
and Institute of Physics, Chinese Academy of Sciences, Beijing 100190, China*

<sup>2</sup>*Collaborative Innovation Center of Quantum Matter, Beijing, China*

<sup>3</sup>*Computational Materials Science Research Team,  
RIKEN Advanced Institute for Computational  
Science (AICS), Kobe, Hyogo 650-0047, Japan*

<sup>4</sup>*New Industry Creation Hatchery Center,  
Tohoku University, Sendai, 980-8579, Japan*

<sup>5</sup>*Computational Materials Science Unit,  
National Institute for Materials Science (NIMS),  
1-1 Namiki, Tsukuba 305-0044, Ibaraki, Japan*

<sup>6</sup>*Computational Condensed Matter Physics Laboratory,  
RIKEN, Wako, Saitama 351-0198, Japan*

<sup>7</sup>*Computational Quantum Matter Research Team,  
RIKEN Center for Emergent Matter Science (CEMS), Wako, Saitama 351-0198, Japan*

<sup>8</sup>*Thermophysics Institute, Siberian Branch,  
Russian Academy of Sciences, Russia*

(Dated: July 7, 2015)

## Abstract

Two-dimensional (2D) topological insulator (TI) have been recognized as a new class of quantum state of matter. They are distinguished from normal 2D insulators with their nontrivial band-structure topology identified by the  $Z_2$  number as protected by time-reversal symmetry (TRS). 2D TIs have intriguing spin-velocity locked conducting edge states and insulating properties in the bulk. In the edge states, the electrons with opposite spins propagate in opposite directions and the backscattering is fully prohibited when the TRS is conserved. This leads to quantized dissipationless "two-lane highway" for charge and spin transportation and promises potential applications. Up to now, only very few 2D systems have been discovered to possess this property. The lack of suitable material obstructs the further study and application. Here, by using first-principles calculations, we propose that the functionalized MXene with oxygen,  $M_2CO_2$  ( $M=W, Mo$  and  $Cr$ ), are 2D TIs with the largest gap of 0.194 eV in  $W$  case. They are dynamically stable and natively antioxidant. Most importantly, they are very likely to be easily synthesized by recent developed selective chemical etching of transition-metal carbides (MAX phase). This will pave the way to tremendous applications of 2D TIs, such as "ideal" conducting wire, multifunctional spintronic device, and the realization of topological superconductivity and Majorana modes for quantum computing.

## I. INTRODUCTION

The field of topological insulator (TI) started from the theoretical proposal of two-dimensional (2D) TI state in graphene.<sup>1-3</sup> Though the band gap of graphene is too tiny to be observed,<sup>4</sup> the conceptual achievement in the band topology has opened the door to the field of topological quantum states (TQs).<sup>5-7</sup> The theoretical proposal<sup>8</sup> and experimental verification<sup>9</sup> of 2D TI in quantum well of HgTe/CdTe have boosted the quick rising of the field of TIs. The idea of band topology has been extended to 3D system<sup>10-12</sup> and other symmetry protected TQs.<sup>13</sup> Recently, the band topology in metals, including the topological Dirac semimetal,<sup>14-17</sup> Weyl semimetal<sup>18-23</sup> and Node-line semimetal,<sup>24-27</sup> has also been intensively studied. Many of the material realization of these TQs are firstly predicted by theoretical calculations and then confirmed by experimental observations.<sup>7,28</sup> The bulk-boundary correspondence of the topological matters is well known now and it is one of the most unique properties of them. For example, 2D TI is expected to host quantum spin Hall effect (QSHE) with 1D helical edge states, namely the electrons in such edge states have opposite velocities in opposite spin channels. Thus, the backscattering is prohibited as long as the perturbation does not break the time-reversal symmetry (TRS). Such helical edge states are expected to serve as "two-lane highway" for dissipationless electron transport, which promises great potential application in low-power and multi-functional spintronic devices. Large band gap 2D TI is also crucial to realize the long-sought-for topological superconductivity and Majorana modes through proximity effect.<sup>6,29</sup> In this point of view, 2D TI is more preferred than 3D one, where the backscattering in the surface states is not fully prohibited.

Compared with the number of well characterized 3D TI materials, fewer 2D TIs have been experimentally discovered.<sup>7,30</sup> The quantum wells of HgTe/CdTe<sup>9</sup> and InAs/GaSb<sup>31</sup> are among the well-known experimentally confirmed 2D TIs. Both of them require precisely controlled MBE growth and operate at ultra-low temperature. These experimental conditions make further studies hard and reduces the possible applications. There have been many efforts to find "good" 2D TIs, which are expected to have the following advantages: (1) being easy to be prepared; (2) having large bulk band gap to be operated under room temperature or higher; (3) being chemically stable upon exposure to air; (4) being composed of cheap and nontoxic elements. The theoretical attempts for predicting good TIs can be roughly classified into two categories. 1) tuning the strength of spin-orbit coupling (SOC),

i.e., the band gap, based on graphene-like honeycomb lattice, such as the low-buckled silicene<sup>32</sup>, chemically decorated single layer honeycomb lattice of Sn,<sup>33</sup> Ge<sup>34</sup> and Bi or Sb,<sup>35</sup> and bucked square lattice BiF<sup>36</sup>. 2) examining new 2D systems, which might be exfoliated from the 3D layered structural materials, such as ZrTe<sub>5</sub>, HfTe<sub>5</sub><sup>37</sup> and Bi<sub>4</sub>Br<sub>4</sub>.<sup>38</sup> Transition-metal dichalcogenide (TMD) in 1T<sup>39</sup> and square-octagon haeckelite<sup>40–42</sup> structure also belong to the later category. None of the above has been confirmed by experiments yet, though ZrTe<sub>5</sub>, HfTe<sub>5</sub> and Bi<sub>4</sub>Br<sub>4</sub> seem to be very promising, since they do exist experimentally and their single layers are TIs without any additional tuning.

Regarding oxide materials, non of them is known to be TI in the experiment, though there are several theoretical proposals available in the literatures, e. g., 2D TI in single layer of iridate Na<sub>2</sub>IrO<sub>3</sub>,<sup>43</sup> topological Mott insulator<sup>44</sup> and Weyl semimetal in pychorelcore A<sub>2</sub>Ir<sub>2</sub>O<sub>7</sub>,<sup>18</sup> axion insulator in spinnel Osmate<sup>45</sup> and 3D TI in perovskite of YBiO<sub>3</sub><sup>46</sup> and heavily doped BaBiO<sub>3</sub>.<sup>47</sup> It is generally believed that the strong electronegativity of oxygen leads to full ionization of cations and results in ionic bonds with large band gap, which makes band inversion difficult. However, the noticeable advantages of oxygen compounds, i.e., naturally antioxidant and stable upon exposure to air, have stimulated continuous efforts in searching for new oxide TIs.

In this paper, by using first-principles calculations we demonstrate that the functionalized MXenes<sup>48–50</sup> with oxygen, M<sub>2</sub>CO<sub>2</sub> with M=W, Mo and Cr, are 2D TIs. Our phonon calculations indicate that the crystal structures are dynamically stable. The band inversion, which is crucial to the nontrivial band topology, is found to occur among the bonding and anti-bonding states of M *d*-orbitals. The results are robust against the use of different exchange-correlation functional approximations. The bulk band gap of W<sub>2</sub>CO<sub>2</sub> is as large as 0.194 eV within generalized gradient approximation (GGA) and is enhanced to 0.472 eV within hybrid functional (HSE06).<sup>51,52</sup> Its *Z*<sub>2</sub> invariant is 1 and has conducting helical edge states. Recently, the 2D material MXene have been successfully obtained by the selective chemical etching of MAX phases — M<sub>*n*+1</sub>AX<sub>*n*</sub> (*n*=1, 2, 3, ...), where M, A and X are a transition metal, an element of group 12-14, C or N, respectively.<sup>53</sup> The bare surfaces of MXene sheet are chemically active and are usually terminated by some atoms or chemical groups depending on the synthesis process, which are usually fluorine (F), oxygen (O), or hydroxyl (OH).<sup>54–56</sup> Therefore, we believe that our proposed M<sub>2</sub>CO<sub>2</sub> can be probably realized experimentally in the future and thus, will advance the application of TI greatly.

TABLE I: The total energies (in eV per unit cell) for the six possible configurations of  $W_2CO_2$ ,  $Mo_2CO_2$  and  $Cr_2CO_2$ . For each configuration, the structure is fully relaxed. In each unit cell, two oxygen atoms are required for full surface saturations. The symbols T, A, and B indicate three different absorption sites of oxygen atoms as depicted in Fig. 1. All calculations here are performed without spin polarization and within GGA.

sites of Oxygen	$W_2CO_2$	$Mo_2CO_2$	$Cr_2CO_2$
TT	3.162	2.779	1.790
AA	1.189	1.112	0.618
TB	1.828	1.782	1.370
TA	2.024	1.733	1.034
<b>BB</b>	<b>0.0</b>	<b>0.0</b>	<b>0.0</b>
BA	0.878	0.698	0.329

## II. COMPUTATIONAL DETAILS

First-principles calculations were carried out by using the Vienna *ab initio* simulation package (VASP)<sup>57,58</sup>. Exchange-correlation potential was treated within the generalized gradient approximation (GGA) of Perdew-Burke-Ernzerhof type.<sup>59</sup> SOC was taken into account self-consistently. The cut-off energy for plane wave expansion is 500 eV and the k-point sampling grid in the self-consistent process was  $12 \times 12 \times 1$ . The crystal structures have been fully relaxed until the residual forces on each atom becomes less than  $0.001 \text{ eV}/\text{\AA}$ . A vacuum of  $20 \text{ \AA}$  between layers was considered in order to minimize the interactions between the layer with its periodic images. PHONOPY has been employed to calculate the phonon dispersion<sup>60</sup>. Considering the possible underestimation of band gap within GGA, non-local Heyd-Scuseria-Ernzerhof (HSE06) hybrid functional<sup>51,52</sup> is further supplemented to check the band topology. To explore the edge states, we apply the Green's function method<sup>7</sup> based on the tight-binding model with the maximally localized Wannier functions (MLWF)<sup>61,62</sup> of  $d$  orbitals of M and  $p$  orbitals of C and O as basis set. MLWF are generated by using the software package OpenMX.<sup>63,64</sup>

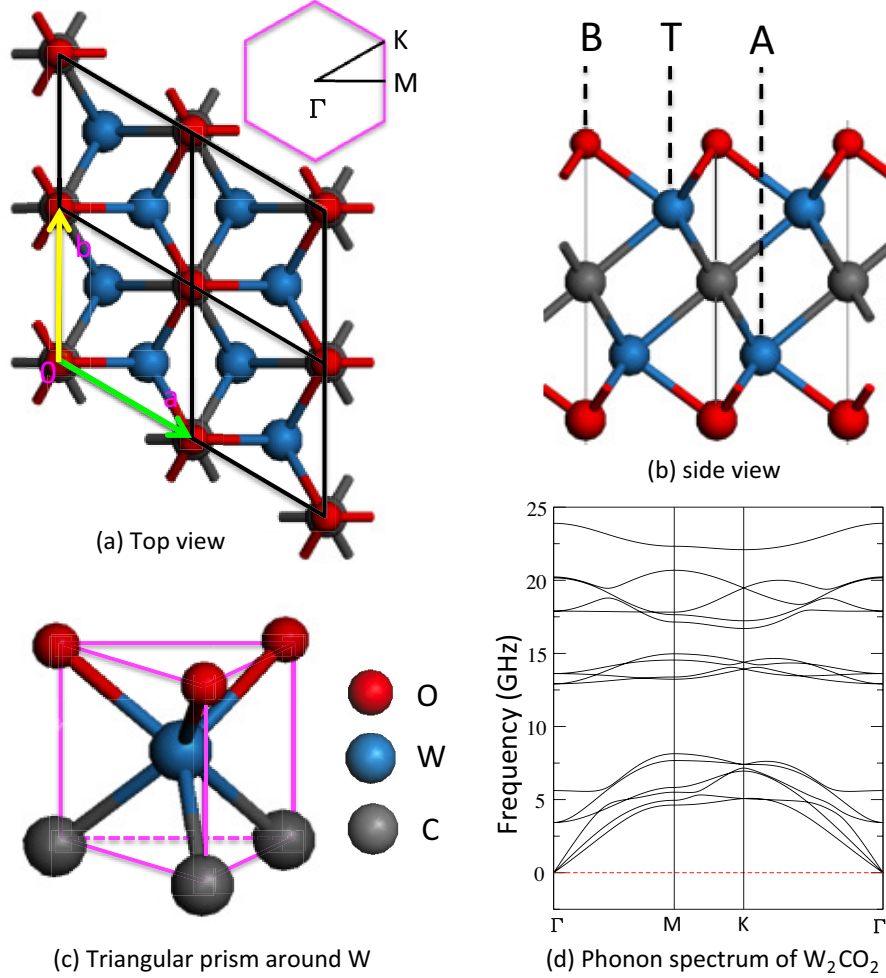


FIG. 1: (Color online) (a) Top view and (b) side view of optimized crystal structure of  $W_2CO_2$  and its 2D Brillouin zone. There are three possible sites for oxygen decoration on either side of the surface, namely B (on top of C site), T (on top of W in top surface), A (on top of W in bottom surface). (c) The triangular prism formed by O and C ions surrounds W. (d) The phonon spectrum for optimized  $W_2CO_2$ .

### III. RESULTS AND DISCUSSION

The crystal structure of oxygen functionalized MXene is shown in Fig. 1. Bare MXene  $M_2C$  is basically a three-layer structure with trigonal lattice. The C atoms form a layer, which is sandwiched between two M layers. The in-plane sites of M atoms are  $(1/3, 2/3)$  and  $(2/3, 1/3)$ , respectively, of the trigonal lattice of C atoms. The bare surfaces of MXene sheet are basically terminated by M atoms and they are chemically reactive. Usually, the surfaces are terminated by F, O or OH depending on the synthesis process. This brings a chance to

tune the electronic properties of MXene by appropriate surface functionalization.<sup>55,56</sup> It has previously been shown that the MXenes with the full surface functionalizations are thermodynamically more favorable than the partial functionalizations,<sup>55</sup> where the full surface functionalization requires two chemical groups per cell. As shown in Fig. 1, the oxygen atom might occupy three different sites on the surface, namely A, B and T on each surface. Therefore, there are totally six combinations for decoration of two surfaces as listed in Table. I. For each case, the crystal structure is fully relaxed and the results of total energy calculations are summarized in Table. I. It is observed that the MXene with BB-type oxygen functionalization obtain the lowest energy. In this configuration the M atom sits inside of a trigonal prism formed by the surrounding C and O, which is very similar to Mo atom in 1H structure of MoS<sub>2</sub>. The phonon spectrum of the energetically stable crystal structure is calculated and shown in Fig. 1(d). Obviously, there is no imaginary frequency, which means such structures are also dynamically stable.

The electronic band structure of W<sub>2</sub>CO<sub>2</sub> is shown in Fig. 2. It is found that there is a degenerate band touch point on the Fermi level when SOC is not considered. These degenerate states are mostly composed of  $d_{x^2-y^2}$  and  $d_{xy}$  orbitals of W atoms as shown by the fat-band analysis. If SOC is further considered, it becomes an insulator. Since it has inversion symmetry, the parity configuration of occupied bands at four time-reversal invariant momenta in the 2D BZ can be easily obtained and the  $Z_2$  invariant is found to be 1. This indicates that W<sub>2</sub>CO<sub>2</sub> is a 2D topological insulator with an indirect band gap as large as 0.194 eV. The topologically protected conducting edge states have Dirac cone like dispersion and connect the bulk valence and conduction bands.

The total and projected partial density of states, as well as the fat-band plot, clearly show that around Fermi level the W  $d$  orbitals are dominant around the Fermi level. The  $p$  orbitals of C and O are mainly located -2 eV below the Fermi level. The five  $d$  orbitals of W atom are within the triangular prism crystal field of  $C_{3v}$  symmetry. The  $d_{xz}$  and  $d_{yz}$  orbitals are double degenerate and are higher in energy due to the strong hybridization with the  $p$  orbitals of C and O. The  $d_{x^2-y^2}$  and  $d_{xy}$  orbitals are also degenerate and they are around the Fermi level. The  $d_{z^2}$  orbital has quite weak hybridization with ligand elements since it points to the center of the ligand triangle. It is also around the Fermi level and slightly lower than  $d_{x^2-y^2}+d_{xy}$ . Therefore, in order to uncover the low-energy physics of W<sub>2</sub>CO<sub>2</sub>, we just need to take into account three  $d$  orbitals,  $d_{x^2-y^2}$ ,  $d_{xy}$  and  $d_{z^2}$ , of the

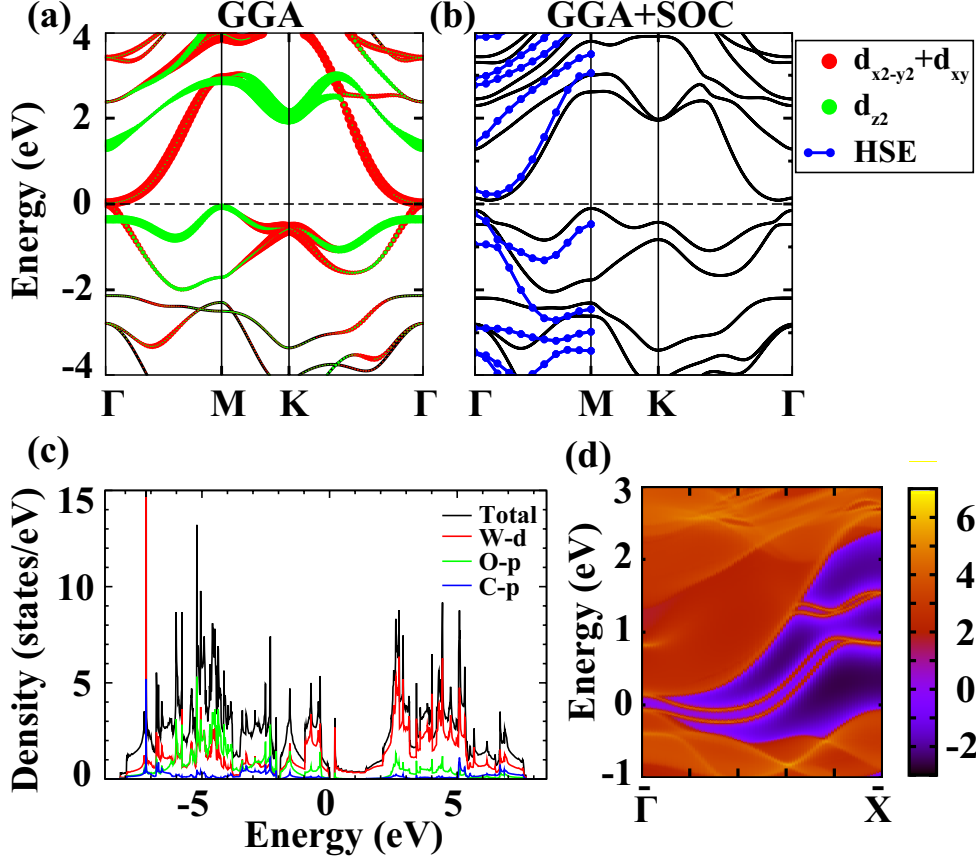


FIG. 2: (Color online) Band structure for  $W_2CO_2$  calculated (a) without and (b) with spin-orbit coupling (SOC). The fat-bands are scaled with the projected weight of different atomic orbitals within the eigenstates as shown in (a). The comparison with the bands from hybrid functional (HSE06) calculation including SOC is shown in (b). Total and projected partial density of states are shown in (c). The edge states along lattice constant  $a$  is shown in (d).

W atoms. It is noticeable that there are two W atoms in one unit cell. As shown in Fig. 3, the above selected  $d$  atomic orbitals form bonding and anti-bonding states. The bonding and anti-bonding states of  $d_{z^2}$  orbitals are even ( $A_{1g}$ ) and odd ( $A_{2u}$ ), respectively. Similarly, those from  $d_{x^2-y^2}+d_{xy}$  are even ( $E_g$ ) and odd ( $E_u$ ) but having double degeneracy. The band inversion happens between the double degenerate  $E_g$  and non-degenerate  $A_{2u}$  states, which brings the nontrivial topology of bands. When the banding effect is considered from  $\Gamma$  to M, the double degenerate  $E_g$  states are split and there is no other band inversion happens. Further, the SOC introduces the spin degree of freedom and it opens a gap around Fermi level as shown in Fig. 1. Due to the heavy W element, the band gap is found to be as large



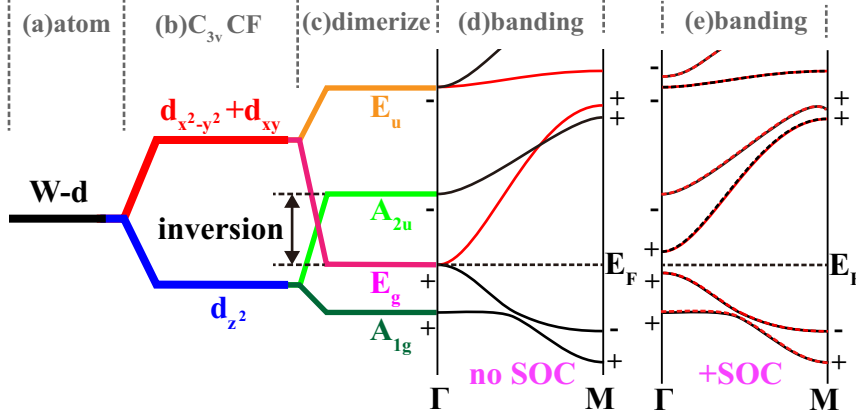


FIG. 3: (Color online) The band inversion mechanism in  $W_2CO_2$ . (a) W 5d orbitals are split (b) under  $C_{3v}$  crystal field (CF) with double degenerate  $d_{x^2-y^2}+d_{xy}$  and single degenerate  $d_{z^2}$  orbitals around Fermi level  $E_F$ . (c) The dimerization of two W atoms in each unit cell leads to bonding and anti-bonding states and band inversion between states with different parities (labeled by + and -). (d) The band dispersion along  $\Gamma$ -M does not induce other band inversion. (e) Including SOC opens band gap and introduces spin degeneracy in each band, with dashed and solid line representing opposite spin channels.

as 0.194 eV. Considering the possible underestimation of the band gaps within GGA, the hybrid functional (HSE06) calculation is used to check whether the above band inversion around  $\Gamma$  is robust. It is found that the band inversion is kept and the band gap is enhanced to as large as 0.472 eV. Such large band gap 2D TI has an advantage in observing quantum spin Hall effect at room-temperature or higher, which is appropriate for device applications.

For  $Mo_2CO_2$  and  $Cr_2CO_2$ , both of them have the similar crystal structure as  $W_2CO_2$  and are also dynamically stable as seen from the phonon spectra shown in Fig. 4. Since Mo and Cr have weaker SOC than W, they are expected to have narrower band gap than  $W_2CO_2$ . In fact, both of them show band structure of semimetals by having compensated electron and hole Fermi pockets. However, at each k point, one can still find well defined band gap with a curved Fermi level. The assumed occupied bands, as denoted with solid lines in Fig. 4, have the same  $Z_2$  number as  $W_2CO_2$ . Therefore, both of them share the same band topology, as well as the underlying physics, with  $W_2CO_2$ .

Furthermore, we have investigated the correlation effect in  $d$  electrons of transition-metal M. For quite delocalized 5d electrons in W and 4d in Mo, detailed GGA+ $U$  ( $U$  is the

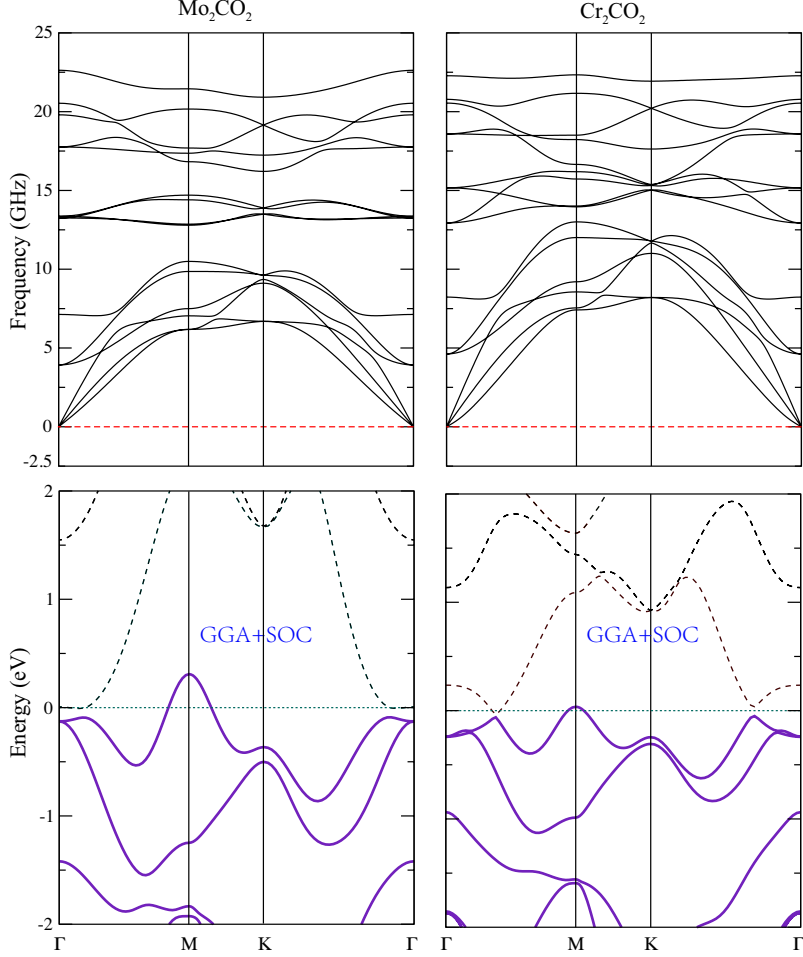


FIG. 4: (Color online) The phonon spectrum (upper panel) and band structure with SOC (lower panel) for optimized stable  $\text{Mo}_2\text{CO}_2$  (left panel) and  $\text{Cr}_2\text{CO}_2$  (right panel) The assumed occupied (unoccupied) bands are denoted with solid (dashed) lines.

parameter for onsite Coulomb interaction) calculations ( $U < 4.0$  eV) show that the correlation effect is negligible and the ground state of  $\text{W}_2\text{CO}_2$  and  $\text{M}_2\text{CO}_2$  are always nonmagnetic. The results discussed above are robust. However, for  $3d$  transition-metal Cr, simple GGA+ $U$  ( $U > 2.0$  eV) calculation for BB configuration gives out solution with magnetic properties. The above non-spin polarization calculations for  $\text{Cr}_2\text{CO}_2$  are helpful to understanding the band gap dependence on the atomic number in that column, but not realistic for  $\text{Cr}_2\text{CO}_2$  itself. However, this gives us the spin degree of freedom in material design based on MXene, which is very crucial to seeking Chern insulators hosting quantum anomalous Hall effect.<sup>65,66</sup> The detailed studies on the dependence of  $U$  value and magnetic configurations are left for future work.

## IV. CONCLUSIONS

Based on the first-principles calculations, we have predicted that a family of oxygen functionalized MXene  $M_2CO_2$  ( $M=W, Mo$  and  $Cr$ ) are 2D TIs. The representative  $W_2CO_2$  has robust band inversion, nontrivial  $Z_2$  invariant and large band gap of 0.194 (0.472) eV within GGA (HSE06). It might satisfy all the four criteria of a "good" 2D TI. (1) easier production process by selective chemical etching method; (2) hosting QSHE at ambient condition; (3) high stability and antioxidant upon exposure to air; and (4) low production cost and consisting of environmental friendly elements.

Inspired by these findings, one can naturally think about obtaining more 2D TI candidates in other functionalized MXenes. The large number of MAX (more than 60)<sup>53,67</sup> brings many possibilities of MXene<sup>50</sup> and huge space in finding topologically nontrivial materials. The possible changes would include replacing  $O^{2-}$  with  $F^-$  or  $(OH)^-$ ,<sup>55,56,68</sup> varying transition-metal  $M$ , replacing  $C$  with  $N$  or  $B$ ,<sup>67</sup> tuning the number of layers  $n$  in MXene  $M_{n+1}C_n$ , etc. The material design or property tailoring with a single or any combination of the above changes will lead to more and better 2D TIs or Chern Insulators.

## V. ACKNOWLEDGMENTS

H.W., Z.F. and X.D. acknowledge the supports from National Natural Science Foundation of China (Grant Nos. 11274359 and 11422428), the National 973 program of China (Grant Nos. 2011CBA00108 and 2013CB921700) and the "Strategic Priority Research Program (B)" of the Chinese Academy of Sciences (Grant No. XDB07020100). H.W. thanks the hospitality during his stay in Tohoku University and part of this work has been done there. Y.K. acknowledges to the Russian Megagrant project (Grant No. 14.B25.31.0030). Both Y.L. and Y.K. are supported by JST, CREST, "A mathematical challenge to a new phase of material sciences" (2008-2013). Partial of the calculations were preformed on TianHe-1(A), the National Supercomputer Center in Tianjin, China.

---

\* Electronic address: hmweng@iphy.ac.cn

- <sup>1</sup> C. L. Kane and E. J. Mele. Quantum spin hall effect in graphene. *Phys. Rev. Lett.*, 95:226801, Nov 2005.
- <sup>2</sup> C. L. Kane and E. J. Mele.  $Z_2$  topological order and the quantum spin hall effect. *Physical Review Letters*, 95(14):146802, September 2005.
- <sup>3</sup> B. Andrei Bernevig and Shou-Cheng Zhang. Quantum spin hall effect. *Physical Review Letters*, 96(10):106802, March 2006.
- <sup>4</sup> Yugui Yao, Fei Ye, Xiao-Liang Qi, Shou-Cheng Zhang, and Zhong Fang. Spin-orbit gap of graphene: First-principles calculations. *Phys. Rev. B*, 75:041401, Jan 2007.
- <sup>5</sup> M Z Hasan and C L Kane. Colloquium: topological insulators. *Rev. Mod. Phys.*, 82(4):3045, 2010.
- <sup>6</sup> X L Qi and S C Zhang. Topological insulators and superconductors. *Rev. Mod. Phys.*, 83(4):1057, 2011.
- <sup>7</sup> Hongming Weng, Xi Dai, and Zhong Fang. Exploration and prediction of topological electronic materials based on first-principles calculations. *MRS Bulletin*, 39:849–858, 10 2014.
- <sup>8</sup> B. Andrei Bernevig, Taylor L. Hughes, and Shou-Cheng Zhang. Quantum Spin Hall Effect and Topological Phase Transition in HgTe Quantum Wells. *Science*, 314(5806):1757–1761, December 2006.
- <sup>9</sup> Markus König, Steffen Wiedmann, Christoph Brüne, Andreas Roth, Hartmut Buhmann, Laurens W. Molenkamp, Xiao-Liang Qi, and Shou-Cheng Zhang. Quantum Spin Hall Insulator State in HgTe Quantum Wells. *Science*, 318(5851):766–770, November 2007.
- <sup>10</sup> Liang Fu, C Kane, and E Mele. Topological Insulators in Three Dimensions. *Physical Review Letters*, 98(10):106803, March 2007.
- <sup>11</sup> J. E. Moore and L. Balents. Topological invariants of time-reversal-invariant band structures. *Phys. Rev. B*, 75:121306, Mar 2007.
- <sup>12</sup> Rahul Roy.  $Z_2$  classification of quantum spin hall systems: An approach using time-reversal invariance. *Phys. Rev. B*, 79:195321, May 2009.
- <sup>13</sup> C.-K. Chiu, J. C. Y. Teo, A. P. Schnyder, and S. Ryu. Classification of topological quantum matter with symmetries. *cond-mat:1505.03535*, May 2015.
- <sup>14</sup> Zhijun Wang, Yan Sun, Xing-Qiu Chen, Cesare Franchini, Gang Xu, Hongming Weng, Xi Dai, and Zhong Fang. Dirac semimetal and topological phase transitions in  $A_3\text{Bi}$  ( $A=\text{Na}, \text{K}, \text{Rb}$ ). *Physical Review B*, 85(19):195320, May 2012.

- <sup>15</sup> Zhijun Wang, Hongming Weng, Quansheng Wu, Xi Dai, and Zhong Fang. Three-dimensional dirac semimetal and quantum transport in  $\text{Cd}_3\text{As}_2$ . *Physical Review B*, 88(12):125427, September 2013.
- <sup>16</sup> Z. K. Liu, B. Zhou, Y. Zhang, Z. J. Wang, Hongming Weng, D. Prabhakaran, S.-K. Mo, Z. X. Shen, Z. Fang, X. Dai, Z. Hussain, and Y. L. Chen. Discovery of a three-dimensional topological dirac semimetal,  $\text{Na}_3\text{Bi}$ . *Science*, 343(6173):864–867, 2014.
- <sup>17</sup> Z K Liu, J Jiang, B Zhou, Z J Wang, Y Zhang, H M Weng, D Prabhakaran, S K Mo, H Peng, P Dudin, T Kim, M Hoesch, Z Fang, X Dai, Z.-X. Shen, D. L. Feng, Z Hussain, and Y L Chen. A stable three-dimensional topological Dirac semimetal  $\text{Cd}_3\text{As}_2$ . *Nature Materials*, 13:677–681, May 2014.
- <sup>18</sup> Xiangang Wan, Ari M. Turner, Ashvin Vishwanath, and Sergey Y. Savrasov. Topological semimetal and fermi-arc surface states in the electronic structure of pyrochlore iridates. *Phys. Rev. B*, 83:205101, May 2011.
- <sup>19</sup> Gang Xu, Hongming Weng, Zhijun Wang, Xi Dai, and Zhong Fang. Chern semimetal and the quantized anomalous hall effect in  $\text{HgCr}_2\text{Se}_4$ . *Physical Review Letters*, 107(18):186806, October 2011.
- <sup>20</sup> Hongming Weng, Chen Fang, Zhong Fang, B. A. Bernevig, and X. Dai. Weyl semimetal phase in noncentrosymmetric transition-metal monophosphides. *Phys. Rev. X*, 5:011029, Mar 2015.
- <sup>21</sup> B. Q. Lv, H. M. Weng, B. B. Fu, X. P. Wang, H. Miao, J. Ma, P. Richard, X. C. Huang, L. X. Zhao, G. F. Chen, Z. Fang, X. Dai, T. Qian, and H. Ding. Discovery of Weyl semimetal TaAs. *ArXiv e-prints*, page 1502.04684, February 2015.
- <sup>22</sup> B. Q. Lv, N. Xu, H. M. Weng, J. Z. Ma, P. Richard, X. C. Huang, L. X. Zhao, G. F. Chen, C. Matt, F. Bisti, V. Stokov, J. Mesot, Z. Fang, X. Dai, T. Qian, M. Shi, and H. Ding. Observation of Weyl nodes in TaAs. *ArXiv e-prints*, page 1503.09188, March 2015.
- <sup>23</sup> X. Huang, L. Zhao, Y. Long, P. Wang, D. Chen, Z. Yang, H. Liang, M. Xue, H. Weng, Z. Fang, X. Dai, and G. Chen. Observation of the chiral anomaly induced negative magneto-resistance in 3D Weyl semi-metal TaAs. *ArXiv e-prints*, page 1503.01304, March 2015.
- <sup>24</sup> A. A. Burkov, M. D. Hook, and Leon Balents. Topological nodal semimetals. *Phys. Rev. B*, 84:235126, Dec 2011.
- <sup>25</sup> H. Weng, Y. Liang, Q. Xu, R. Yu, Z. Fang, X. Dai, and Y. Kawazoe. Topological Node-Line Semimetal in Three Dimensional Graphene Networks. *ArXiv e-prints*, page 1411.2175 (accepted)

- by Phys. Rev. B), November 2014.
- <sup>26</sup> R. Yu, H. Weng, Z. Fang, X. Dai, and X. Hu. Topological Nodal Line Semimetal and Dirac Semimetal State in Antiperovskite  $\text{Cu}_3\text{PdN}$ . *ArXiv e-prints*, page 1504.04577 (accepted by Phys. Rev. Lett.), April 2015.
- <sup>27</sup> Y. Kim, B. J. Wieder, C. L. Kane, and A. M. Rappe. Dirac Line Nodes in Inversion Symmetric Crystals. *ArXiv e-prints*, page 1504.03807, April 2015.
- <sup>28</sup> Haijun Zhang and Shou-Cheng Zhang. Topological insulators from the perspective of first-principles calculations. *physica status solidi (RRL) - Rapid Research Letters*, 7(1-2):72–81, February 2013.
- <sup>29</sup> Liang Fu and C. L. Kane. Superconducting proximity effect and majorana fermions at the surface of a topological insulator. *Phys. Rev. Lett.*, 100:096407, Mar 2008.
- <sup>30</sup> Yoichi Ando. Topological insulator materials. *Journal of the Physical Society of Japan*, 82(10):102001, September 2013.
- <sup>31</sup> Ivan Knez, Rui-Rui Du, and Gerard Sullivan. Evidence for helical edge modes in inverted InAs/GaSb quantum wells. *Phys. Rev. Lett.*, 107:136603, Sep 2011.
- <sup>32</sup> Cheng-Cheng Liu, Wanxiang Feng, and Yugui Yao. Quantum Spin Hall Effect in Silicene and Two-Dimensional Germanium. *Physical Review Letters*, 107(7):076802, August 2011.
- <sup>33</sup> Yong Xu, Binghai Yan, Hai-Jun Zhang, Jing Wang, Gang Xu, Peizhe Tang, Wenhui Duan, and Shou-Cheng Zhang. Large-gap quantum spin hall insulators in tin films. *Phys. Rev. Lett.*, 111:136804, Sep 2013.
- <sup>34</sup> Chen Si, Junwei Liu, Yong Xu, Jian Wu, Bing-Lin Gu, and Wenhui Duan. Functionalized germanene as a prototype of large-gap two-dimensional topological insulators. *Phys. Rev. B*, 89:115429, Mar 2014.
- <sup>35</sup> Z. Song, C.-C. Liu, J. Yang, J. Han, M. Ye, B. Fu, Y. Yang, Q. Niu, J. Lu, and Y. Yao. Quantum spin hall insulators and quantum valley hall insulators of  $\text{BiX/SbX}$  ( $X=\text{H, F, Cl}$  and  $\text{Br}$ ) monolayers with a record bulk band gap. *NPG Asia Materials*, 6:e147, December 2014.
- <sup>36</sup> Wei Luo and Hongjun Xiang. Room temperature quantum spin hall insulators with a buckled square lattice. *Nano Letters*, 15(5):3230–3235, 2015.
- <sup>37</sup> Hongming Weng, Xi Dai, and Zhong Fang. Transition-metal pentatelluride  $\text{ZrTe}_5$  and  $\text{HfTe}_5$ : A Paradigm for Large-Gap Quantum Spin Hall Insulators. *Physical Review X*, 4(1):011002, January 2014.

- <sup>38</sup> Jin-Jian Zhou, Wanxiang Feng, Cheng-Cheng Liu, Shan Guan, and Yugui Yao. Large-Gap Quantum Spin Hall Insulator in Single Layer Bismuth Monobromide Bi<sub>4</sub>Br<sub>4</sub>. *Nano Letters*, 14(8):4767–4771, August 2014.
- <sup>39</sup> Xiaofeng Qian, Junwei Liu, Liang Fu, and Ju Li. Quantum spin hall effect in two-dimensional transition metal dichalcogenides. *Science*, 346(6215):1344–1347, 2014.
- <sup>40</sup> S. M. Nie, Zhida Song, Hongming Weng, and Zhong Fang. Quantum spin hall effect in two-dimensional transition-metal dichalcogenide haeckelites. *Phys. Rev. B*, 91:235434, Jun 2015.
- <sup>41</sup> Y. Sun, C. Felser, and B. Yan. Graphene-like Dirac states and Quantum Spin Hall Insulators in the square-octagonal MX<sub>2</sub> (M=Mo, W; X=S, Se, Te) Isomers. *ArXiv e-prints*, page 1503.08460, March 2015.
- <sup>42</sup> Y. Ma, L. Kou, Y. Dai, and T. Heine. Quantum Spin Hall Effect and Topological Phase Transition in Two-Dimensional Square Transition Metal Dichalcogenides. *ArXiv e-prints*, page 1504.00197, April 2015.
- <sup>43</sup> Atsuo Shitade, Hosho Katsura, Jan Kuneš, Xiao-Liang Qi, Shou-Cheng Zhang, and Naoto Nagaosa. Quantum spin hall effect in a transition metal oxide na<sub>2</sub>iro<sub>3</sub>. *Phys. Rev. Lett.*, 102:256403, Jun 2009.
- <sup>44</sup> Dmytro Pesin and Leon Balents. Mott physics and band topology in materials with strong spin-orbit interaction. *Nature Physics*, 6:376–381, March 2010.
- <sup>45</sup> Xiangang Wan, Ashvin Vishwanath, and Sergey Y. Savrasov. Computational design of axion insulators based on 5d spinel compounds. *Phys. Rev. Lett.*, 108:146601, Apr 2012.
- <sup>46</sup> Hosub Jin, Sonny H. Rhim, and Arthur J. Freeman. Topological Oxide Insulator in Cubic Perovskite Structure. *Scientific Reports*, 3:1651, April 2012.
- <sup>47</sup> Binghai Yan, Martin Jansen, and Felser Claudia. A large-energy-gap oxide topological insulator based on the superconductor BaBiO<sub>3</sub>. *Nature Physics*, 9:709–711, September 2013.
- <sup>48</sup> Michael Naguib, Murat Kurtoglu, Volker Presser, Jun Lu, Junjie Niu, Min Heon, Lars Hultman, Yury Gogotsi, and Michel W. Barsoum. Two-dimensional nanocrystals produced by exfoliation of ti<sub>3</sub>alc<sub>2</sub>. *Adv. Mater.*, 23:4248–4253, 2011.
- <sup>49</sup> Michael Naguib, Olha Mashtalir, Joshua Carle, Volker Presser, Jun Lu, Lars Hultman, Yury Gogotsi, and Michel W. Barsoum. Two-dimensional transition metal carbides. *ACS Nano*, 6(2):1322–1331, 2011.
- <sup>50</sup> Michael Naguib, Vadym N. Mochalin, Michel W. Barsoum, and Yury Gogotsi. 25th anniversary

- article: Mxenes: A new family of two-dimensional materials. *Adv. Mater.*, 26:992–1005, 2014.
- <sup>51</sup> Jochen Heyd, Gustavo E Scuseria, and Matthias Ernzerhof. Hybrid functionals based on a screened coulomb potential. *The Journal of Chemical Physics*, 118(18):8207–8215, 2003.
- <sup>52</sup> Jochen Heyd, Gustavo E Scuseria, and Matthias Ernzerhof. Erratum: "hybrid functionals based on a screened coulomb potential" [j. chem. phys. 118, 8207 (2003)]. *The Journal of Chemical Physics*, 124(21):219906, 2006.
- <sup>53</sup> Michel W. Barsoum. The  $m_{n+1}ax_n$  phases: A new class of solids: Thermodynamically stable nanolaminates. *Progress in Solid State Chemistry*, 28(1&A54):201 – 281, 2000.
- <sup>54</sup> Kristopher J. Harris, Matthieu Bugnet, Michael Naguib, Michel W. Barsoum, and Gillian R. Goward. Direct measurement of surface termination groups and their connectivity in the 2d mxene v2ctx using nmr spectroscopy. *The Journal of Physical Chemistry C*, 119(24):13713–13720, 2015.
- <sup>55</sup> Mohammad Khazaei, Masao Arai, Taizo Sasaki, Chan-Yeup Chung, Natarajan S. Venkataramanan, Mehdi Estili, Yoshio Sakka, and Yoshiyuki Kawazoe. Novel electronic and magnetic properties of two-dimensional transition metal carbides and nitrides. *Adv. Funct. Mater.*, 23:2185–2192, 2013.
- <sup>56</sup> Mohammad Khazaei, Masao Arai, Taizo Sasaki, Mehdi Estili, and Yoshio Sakka. Two-dimensional molybdenum carbides: potential thermoelectric materials of the mxene family. *Phys. Chem. Chem. Phys.*, 16:7841, 2014.
- <sup>57</sup> Georg Kresse and Jürgen Furthmüller. Efficiency of ab-initio total energy calculations for metals and semiconductors using a plane-wave basis set. *Computational Materials Science*, 6(1):15–50, 1996.
- <sup>58</sup> Georg Kresse and Jürgen Furthmüller. Efficient iterative schemes for ab initio total-energy calculations using a plane-wave basis set. *Physical Review B*, 54(16):11169, 1996.
- <sup>59</sup> John Perdew, Kieron Burke, and Matthias Ernzerhof. Generalized gradient approximation made simple. *Phys. Rev. Lett.*, 77:3865–3868, Oct 1996.
- <sup>60</sup> Atsushi Togo, Fumiyasu Oba, and Isao Tanaka. First-principles calculations of the ferroelastic transition between rutile-type and cacl 2-type sio 2 at high pressures. *Physical Review B*, 78(13):134106, 2008.
- <sup>61</sup> Nicola Marzari and David Vanderbilt. Maximally localized generalized wannier functions for composite energy bands. *Physical review B*, 56(20):12847, 1997.



- <sup>62</sup> Ivo Souza, Nicola Marzari, and David Vanderbilt. Maximally localized wannier functions for entangled energy bands. *Physical Review B*, 65(3):035109, 2001.
- <sup>63</sup> <http://www.openmx-square.org>.
- <sup>64</sup> Hongming Weng, Taisuke Ozaki, and Kiyoyuki Terakura. Revisiting magnetic coupling in transition-metal-benzene complexes with maximally localized wannier functions. *Phys. Rev. B*, 79:235118, Jun 2009.
- <sup>65</sup> Rui Yu, Wei Zhang, Hai-Jun Zhang, Shou-Cheng Zhang, Xi Dai, and Zhong Fang. Quantized anomalous hall effect in magnetic topological insulators. *Science*, 329(5987):61–64, 2010.
- <sup>66</sup> Cui-Zu Chang, Jinsong Zhang, Xiao Feng, Jie Shen, Zuo Cheng Zhang, Minghua Guo, Kang Li, Yunbo Ou, Pang Wei, Li-Li Wang, Zhong-Qing Ji, Yang Feng, Shuaihua Ji, Xi Chen, Jinfeng Jia, Xi Dai, Zhong Fang, Shou-Cheng Zhang, Ke He, Yayu Wang, Li Lu, Xu-Cun Ma, and Qi-Kun Xue. Experimental observation of the quantum anomalous hall effect in a magnetic topological insulator. *Science*, 340(6129):167–170, 2013.
- <sup>67</sup> Mohammad Khazaei, Masao Arai, Taizo Sasaki, Mehdi Estili, and Yoshio Sakka. Trends in electronic structures and structural properties of max phases: a first-principles study on  $m^2$  alc ( $m = \text{sc, ti, cr, zr, nb, mo, hf, or ta}$ ),  $m^2$  aln, and hypothetical  $m^2$  alb phases. *Journal of Physics: Condensed Matter*, 26(50):505503, 2014.
- <sup>68</sup> H. Fashandi, V. Ivády, P. Eklund, A. Lloyd Spetz, M. I. Katsnelson, and I. A. Abrikosov. Dirac points with giant spin-orbit splitting in the electronic structure of two-dimensional transition-metal carbides. *ArXiv e-prints*, page 1506.05398, June 2015.